Dyes and Pigments 95 (2012) 679–688

Contents lists available at SciVerse ScienceDirect

Dyes and Pigments

journal homepage: www.elsevier.com/locate/dyepig

# The synthesis, photophysical and electrochemical properties of a series of novel 3,8,13-substituted triindole derivatives

Tianhao Zhu [a], Guangke He [a], Jin Chang [b], Dongdong Zhao [a], Xiaolin Zhu [a], Hongjun Zhu [a,*]

[a] Department of Applied Chemistry, College of Science, Nanjing University of Technology, Nanjing 210009, PR China
[b] Discipline of Chemistry, Queensland University of Technology, 2 George St., Brisbane, QLD 4000, Australia

ARTICLE INFO

*Article history:*
Received 17 April 2012
Received in revised form
16 June 2012
Accepted 18 June 2012
Available online 4 July 2012

*Keywords:*
Synthesis
Optical properties
Electrochemical properties
Triindoles
Quantum chemical calculations
Organic light-emitting diodes (OLEDs)

ABSTRACT

The synthesis and properties of a series of new 3,8,13-substituted triindole derivatives **1a**–**1e** are reported. The 3,8,13-substituted triindoles were thermally robust with high decomposition temperatures (≥405 °C) and high melt transitions (219 °C–373 °C). Compound **5e** was crystallized in the monoclinic system with the space group $P2_1/n$. These compounds showed UV–Vis absorption ($\lambda_{max}^{Abs}$) in the range of 311–345 nm in DCM solution and 371–391 nm in solid state, and fluorescence maxima ($\lambda_{max}^{Em}$) in the range of 394–412 nm in DCM solution and 416–461 nm in solid state. The fluorescence quantum yields ranged from 0.27 to 0.58. The estimated electron affinities (LUMO levels) and estimated ionization potential (HOMO levels) of compounds **1a**–**1e** are 3.54–3.71 eV and 5.12–5.48 eV, respectively. Quantum chemical calculations using DFT B3LYP/6-31G showed nearly identical LUMO (−0.72 to −1.10 eV) and HOMO (−4.65 to −4.84 eV) values. These results demonstrated that the new 3,8,13-substituted triindoles are promising thermally stable host materials for organic light-emitting diodes with reasonable hole mobility.



## 1. Introduction

The field of organic electronics developed rapidly in the last few years. Compared to conventional inorganic crystalline semiconductors, organic light-emitting diodes (OLEDs) aroused worldwide interest in the search for alternative properties for large area, flexible, lightweight, and energy efficient optoelectronics [1,2]. π-conjugated materials are extensively investigated and explored for OLEDs because of their potential in the creation of cost-effective, power-efficient, and eventually, flexible electronic devices [3–5]. Tang and VanSlyke first reported the use of multilayer OLEDs [6]. Among the many factors that determine the performance of OLEDs, the most important is in relation to the charge balance factor for the injection and transport of electrons and holes to the recombination zone in the hole-transport layer [7–9]. Nowadays, aromatic cores with a large π-orbital area attract interest as well. These molecules have a strong tendency to assemble in highly ordered organizations caused by stacking, which paves the way for a favorable overlap of π-orbitals, and consequently, for improved hole-transport properties [10–12].

Carbazolyl groups are well-known hole-transporting units because of the electron-donating capabilities associated with the nitrogen atom. Their good charge-transport properties and carbazole-related materials are already utilized in a number of applications [13,14]. Nowadays, researchers are interested in the electron-rich 10,15-dihydro-5H-diindolo [3,2-a:30,20-c] carbazole (triindole), which is an extended π-system constituting three carbazole units that share an aromatic ring. Hence, interesting and special functional properties are expected from its derivatives, which have acquired several applications in hole-transporting materials, discotic liquid crystals, and OLEDs [15–17].

Some triindole derivatives were synthesized using the triindole core as a precursor [18]. The synthetic approach to obtain the triindole core is the cyclocondensation of either indolin-2-one [19] or indole itself [20] through halogenation. However, whether triindole derivatives can be synthesized directly by trimerization of aryl derivatives of indolin-2-one remains unknown.

In this context we report a series of novel 3,8,13-substituted triindoles synthesized by trimerization of derivatives of indolin-2-one containing various aromatic substituents. Their photophysical and electrochemical properties were investigated with the aim of understanding structural–physical property relationships in novel organic light-emitting materials.

* Corresponding author. Tel.: +86 25 83172358; fax: +86 25 83587443.
*E-mail address:* zhuhjnjut@hotmail.com (H. Zhu).

0143-7208/$ – see front matter © 2012 Elsevier Ltd. All rights reserved.
http://dx.doi.org/10.1016/j.dyepig.2012.06.011

## 2. Experimental section

### 2.1. Materials

*N*-Ethylaniline was purchased from Shanghai Wison Engineering and Technology Co. Ltd. Fluorene and N-bromosuccinimide were purchased from Beijing Rizhaoshilide Chemical Company. 1-Bromo-4-tert-butylbenzene and 1-bromo-4-methoxybenzene were purchased from Qing Zhou Shi Ao Xing Hua Gong Co. Ltd. $Pd(OAc)_2$ was purchased from Shanghai Yu Rui Chemical Co. Ltd. $POCl_3$ was purchased from Sandong Chunguang Chemical Science and Technology. Co. Ltd. Tetrahydrofuran (THF) were refluxed with sodium and distilled. Other reagents and solvents were purchased from Sinopharm Chemical Reagent Co. Ltd. and used as received. 5-Bromo-N-ethyloxindole **3** [21], aryl boronic acid compounds **4a**–**4c** [22], **4d** [23] and **4e** [24], indolin-2-one derivatives **5a**–**5e** [25] and 3,8,13-substituted 10,15-dihydro-5H-diindolo[3,2-a:30,20-c]carbazole (triindole) derivatives **1a**–**1e** [21] were synthesized according to the methods reported in literature with some modification. The synthetic routines are shown in Schemes 1 and 2, respectively.

### 2.2. Measurements

$^1H$ NMR and $^{13}C$ NMR spectra were recorded on a Bruker AV-500 spectrometer at 500 MHz, a Bruker AV-400 spectrometer at 400 MHz or a Bruker AV-300 spectrometer at 300 MHz with tetramethylsilane as internal standard. Mass spectra were obtained on a VG12-250 mass spectrometer. Thermogravimetric analysis (TGA) of the molecules and differential scanning calorimetry (DSC) were conducted on a TA Instruments NETZSCH TG 209 and a DSC Instruments NETZSCH DSC 204, respectively. Optical absorption spectra were obtained by using a HP-8453 UV/Vis/near-IR Spectrophotometer (Agilent). Photoluminescence spectra were carried out on a LS-55 spectrofluorometer (Perkin–Elmer). Cyclic voltammetry (CV) was carried out using a CHI 440A electrochemistry workstation (CHI USA) with platinum electrodes at a scan rate of 40 mV/s against an $Ag/Ag^+$ reference electrode. An electrolyte solution of 0.1 M TBAP in DCM was used in all experiments [26].

### 2.3. Synthesis

#### 2.3.1. *N-Ethyloxindole* ***2***

*N*-Ethylaniline (22 g, 182 mmol) was dissolved in toluene (250 mL), and chloroacetyl chloride (14.5 mL, 193 mmol) was added dropwise. Then the mixture was refluxed for 2 h. Water (50 mL) was added after the mixture was cooled to room temperature and the mixture was stirred for 3 h to decompose the chloroacetyl chloride. Toluene layer was washed first with 10% $K_2CO_3$ in water solution, then with HCl (2 M) before dried overnight with sodium sulfate. After toluene was evaporated, $AlCl_3$ (83 g) was added, and the mixture was stirred for 10 min at 130 °C. Then the above mixture was stirred at 210 °C for 45 min. The reaction mixture was poured into quick-stirring ice water slowly, and then condensed HCl (50 mL) was added. The mixture was extracted with 300 mL DCM for three times, and then the DCM layer was dried over sodium sulfate, after DCM was evaporated, the solid was recrystallized with hexane, got N-ethyloxindole **2** (20.3 g) in total yield 76% of the two steps; m.p. 94–95 °C (lit. [21]: 93–95 °C). $^1H$ NMR ($CDCl_3$, 400 MHz): $\delta$ (ppm): 7.24–7.30 (m, 2H), 7.03 (dd, 1H, $J = 7.2$ Hz), 6.85 (d, 1H, $J = 7.8$ Hz), 3.77 (q, 2H, $J = 7.2$ Hz), 3.53 (s, 2H), 1.27 (t, 3H, $J = 7.2$ Hz).

#### 2.3.2. *5-Bromo-N-ethyloxindole* ***3***

*N*-Ethyloxindole (32.4 g, 185 mmol) in acetonitrile (200 mL) was stirred at −5 °C, and then NBS (34 g, 191 mmol) in 300 mL acetonitrile was added dropwise. The mixture was stirred at that

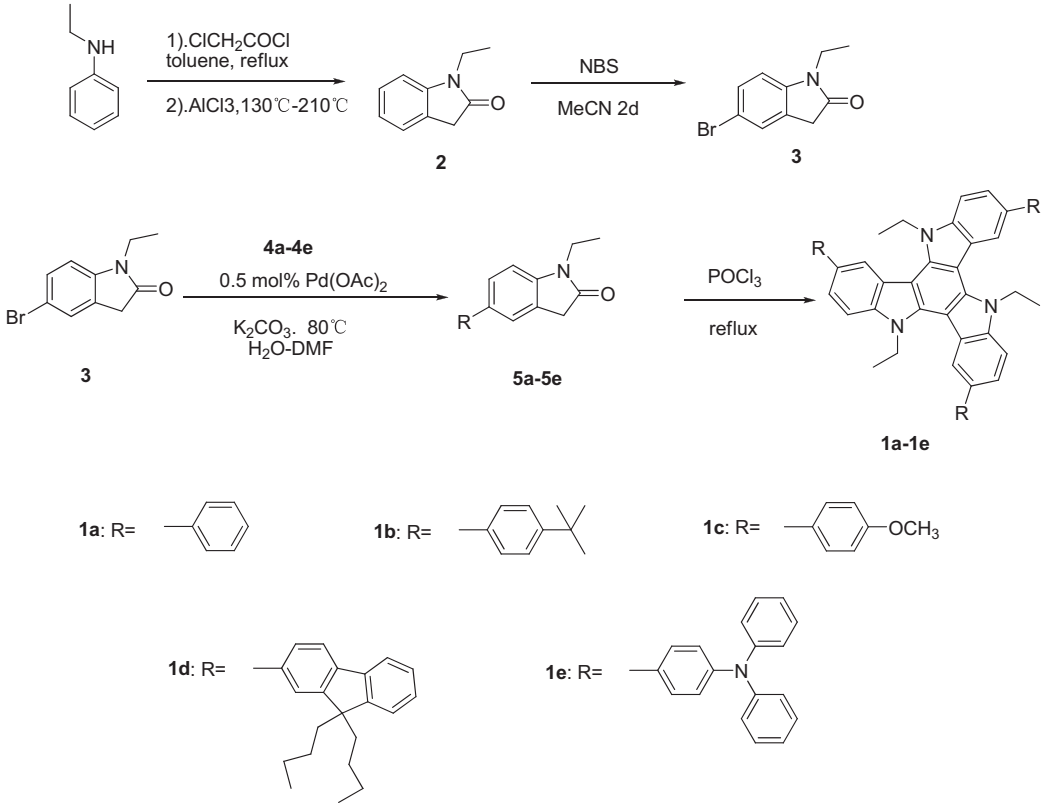


**Scheme 1.** Synthesis of triindole derivatives (**1a**–**1e**).

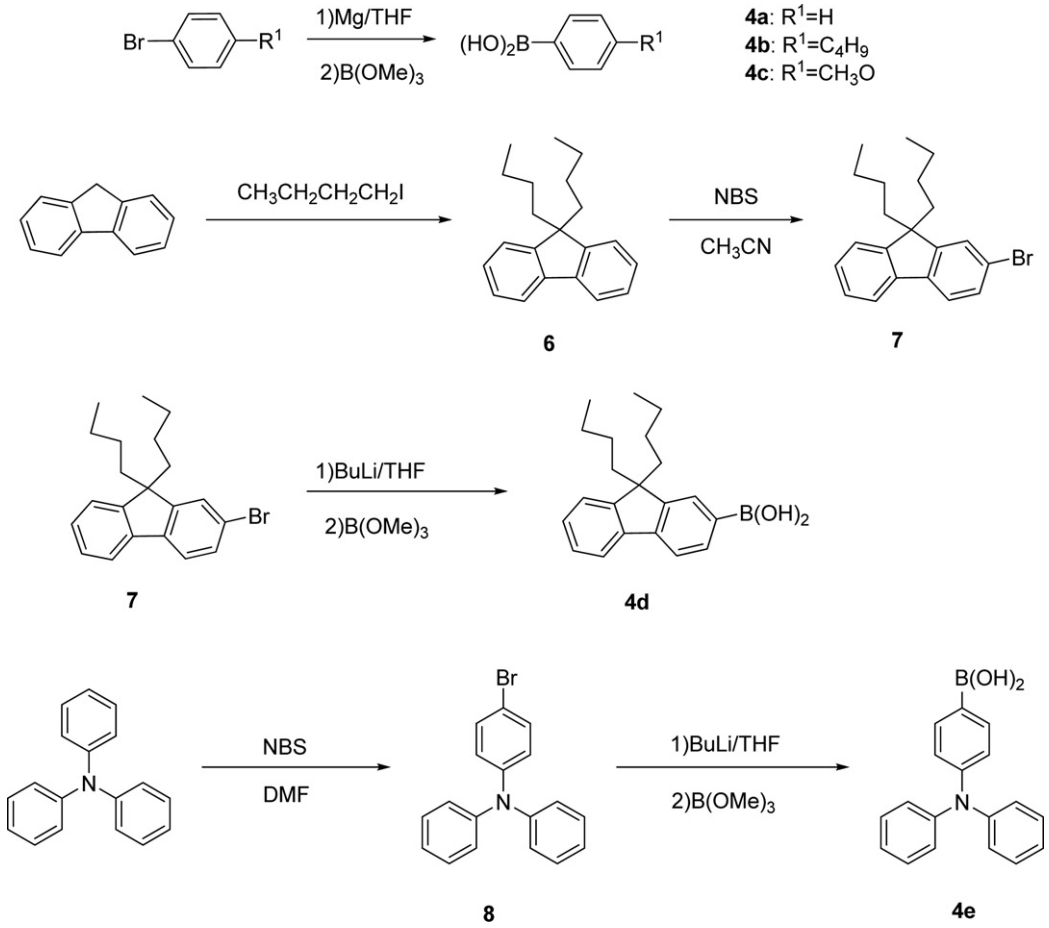


**Scheme 2.** Synthesis of aryl boronic acid compounds (**4a**–**4e**).

temperature for 1 h and then stirred for 2 d at ambient temperature. Then the solution was evaporated and the solid was dissolved in 1000 mL DCM, washed trice with 1000 mL water. After DCM was evaporated, the brown solid was recrystallized with 400 mL isopropyl ether, got 5-bromo-N-ethyloxindole **3** (35.4 g) in 78.9% yield; m.p. 107–109 °C (lit. [21]: 108–109 °C). $^1$H NMR ($CDCl_3$, 400 MHz): $\delta$ (ppm): 7.41 (d, 1H, $J$ = 8.3 Hz), 7.38 (s, 1H), 6.73 (d, 1H, $J$ = 8.2 Hz), 3.75 (m, 2H), 3.51 (s, 2H), 1.26 (t, 3H, $J$ = 7.2 Hz).

*2.3.3. General procedure for the synthesis of (**4a**–**4e**)*

*2.3.3.1. Benzeneboronic acid **4a**.* In a 500 mL Schlenk flask, 4-bromobenzene (450.0 mmol, 70.65 g) in 150 mL THF was added dropwise to magnesium (495.0 mmol, 12.3 g) turnings. The resulting Grignard solution was filtered and added slowly dropwise with stirring to a calculated amount of trimethyl borate (675 mmol, 70.1 g) in 100 mL THF at such a rate that the temperature did not rise above −70 °C. Therefore the flask was cooled using liquid nitrogen. The reaction mixture was poured into quick-stirring ice water slowly, and then condensed HCl (5 mL) was added. After stirring for 30 min, the mixture was shaken repeatedly with ether. The combined organic layers were washed with water, dried over anhydrous sodium sulfate, filtered, and concentrated to dryness. The solid washed with hot hexane, got white solid benzeneboronic acid **4a** (45.2 g). Yield was 82.4%; m.p. 214–218 °C (lit. [27]: 216–219 °C). $^1$H NMR (400 MHz, $CDCl_3$): $\delta$ (ppm): 8.24 (d, 2H, $J$ = 6.8 Hz), 7.59 (t, 1H, $J$ = 7.2 Hz), 7.50 (t, 2H, $J$ = 7.2 Hz).

*2.3.3.2. 4-tert-Butylbenzeneboronic acid **4b**.* Compound **4b** was synthesized according to the method described for compound **4a** Yield was 72.8% as white solid; m.p. 158–160 °C (lit. [22]: 160 °C). $^1$H NMR ($CD_3Cl$, 300 MHz): $\delta$ (ppm): 8.17 (d, 2H, $J$ = 6.6 Hz), 7.42–7.54 (m, 2H), 1.38 (s, 9H).

*2.3.3.3. 4-Methoxyphenylboronic acid **4c**.* Compound **4c** was synthesized according to the method described for compound **4a**. Yield was 75.4% as white solid; m.p. 158–163 °C (lit. [22]: 159–164 °C). $^1$H NMR ($CD_3Cl$, 300 MHz): $\delta$ (ppm): 7.84 (d, 2H, $J$ = 8 Hz), 6.86 (d, 2H, $J$ = 8 Hz), 3.77 (s, 3H).

*2.3.3.4. 9,9-Di(n-butyl)fluorene **6** (lit. [23]).* A mixture of fluorene (33.2 g, 0.2 mol), *n*-butyliodide (80 g, 0.44 mol), and sodium hydroxide (24 g, 0.6 mol) in DMSO (240 mL) was stirred overnight at 90 °C under an inert atmosphere. After cooling to room temperature, the solution was poured into cold water and the resulting mixture was extracted with DCM (3 × 100 mL). The combined organic layers were washed with water, dried over anhydrous sodium sulfate, filtered, and concentrated to dryness. The crude product was then purified by column chromatography on silica gel using petroleum ether as eluent to afford the desired product as a colorless solid **6** (43 g, 76.4% yield); m.p. 55–57 °C. $^1$H NMR (400 MHz, $CDCl_3$): $\delta$ (ppm): 7.69–7.72 (m, 2H), 7.27–7.33 (m, 6H), 1.94–1.98 (m, 4H), 1.03–1.09 (m, 4H), 0.66 (t, 6H, $J$ = 7.4 Hz), 0.54–0.62 (m, 4H).

*2.3.3.5. 9,9-Di(n-butyl)-2-bromofluorene **7** (lit. [23]).* A mixture of 9,9-*Di*(n-butyl)fluorene (26 g, 92 mmol) and NBS (16.5 g, 92 mmol) in acetone (200 mL) was stirred under nitrogen at 80 °C for 3 h. After cooling to room temperature, the solution was poured into

cold water and the resulting mixture was extracted with DCM (3 × 200 mL). The combined organic layers were washed with water, dried over anhydrous sodium sulfate, filtered, and concentrated to dryness. The crude product was purified by short-column chromatography on silica gel using petroleum ether as eluent to afford the desired product as a colorless solid **7** (29.2 g, 92.7% yield); m.p. 58–61 °C. $^1$H NMR (400 MHz, $CDCl_3$): $\delta$ (ppm): 7.64–7.66 (m, 1H), 7.50–7.55 (m, 1H), 7.43–7.47 (m, 2H), 7.31–7.34 (m, 3H), 1.88–1.96 (m, 4H), 1.03–1.12 (m, 4H), 0.68 (t, 6H, $J$ = 7.4 Hz), 0.52–0.63 (m, 4H).

*2.3.3.6. 9,9-Di(n-butyl)-2-ylboronicfluorene acid **4d** (lit. [23]).* In a 250 mL round bottom flask was placed **7** (14.2 g, 40 mmol). The flask was evacuated under vacuum and flushed with nitrogen three times. THF (150 mL) was then added. The mixture was cooled to −78 °C and *n*-BuLi (19.2 mL, 48 mmol) was slowly added. After the mixture was stirred for 5 h at −78 °C, trimethyl borate (5.6 mL, 48 mmol) was injected. After 2 h, the mixture was slowly warmed to room temperature. HCl (3 M, 150 mL) solution was added and the mixture was stirred for another 3 h. The mixture was extracted with DCM three times. The combined organic layers were washed with water, dried over anhydrous sodium sulfate. The product was then dried under high vacuum. The crude product was condensed and purified on a silica-gel column using a mixture of DCM and acetone (5:1 by volume) as eluent. A white solid **4d** (5.83 g, 45.3% yield) was obtained; m.p. 145–148 °C. $^1$H NMR (300 MHz, $d_6$-DMSO): $\delta$ (ppm): 7.98 (s, 2H), 7.83 (s, 1H), 7.74–7.82 (m, 3H), 7.43–7.45 (m, 1H), 7.31–7.34 (m, 2H), 1.95–1.99 (m, 4H), 0.98–1.06 (m, 4H), 0.61 (t, 6H, $J$ = 7.5 Hz), 0.46–0.50 (m, 4H).

*2.3.3.7. 4-Bromo-N,N-diphenylaniline **8**.* A solution of N-bromosuccinimide (35.6 g, 200 mmol) in dry DMF (200 mL) was added to a solution of triphenylamine (49.1 g, 200 mmol) in dry DMF (100 mL) and stirred at 20 °C. After 24 h, the mixture was poured into water (500 mL) and extracted with DCM (3 × 100 mL). The combined organic layers were washed with water, dried over anhydrous sodium sulfate. The product was then dried under high vacuum. After recrystallization from dry ethanol, (48.9 g, 75.3% yield), of the desired product **8** was obtained as a white powder; m.p. 102–104 °C (lit. [24] 102–105 °C). $^1$H NMR (400 MHz, $CDCl_3$): $\delta$ (ppm): 7.30 (m, 6H), 7.06 (m, 6H), 6.94 (m, 2H).

*2.3.3.8. 4-(Diphenylamino)phenylboronic acid **4e**.* In a 500 mL round bottom flask was placed **8** (16.2 g, 50 mmol). The flask was evacuated under vacuum and flushed with nitrogen three times. THF (150 mL) was then added. The mixture was cooled to −78 °C and *n*-BuLi (24 mL, 60 mmol) was slowly added. After the mixture was stirred for 3 h at −78 °C, trimethyl borate (7 mL, 60 mmol) was injected. After 2 h, the mixture was slowly warmed to room temperature. HCl (3 M, 200 mL) solution was added and the mixture was stirred for another 3 h. The mixture was extracted with DCM three times. The combined organic layers were washed with water, dried over anhydrous sodium sulfate. The product was then dried under high vacuum. The crude product was condensed and purified on a silica-gel column using a mixture of chloroform and acetone (4:1 by volume) as eluent. A white solid **4e** (6.6 g, 45.3% yield) was obtained; m.p. 226–228 °C (lit. [24] 228–229 °C). $^1$H NMR (300 MHz, $d_6$-DMSO): $\delta$ (ppm): 7.84 (s, 2H), 7.66 (d, 2H, $J$ = 7.5 Hz), 7.30 (t, 4H, $J$ = 7.8 Hz), 7.02–7.09 (m, 6H), 6.86–6.88 (m, 2H).

*2.3.4. General procedure for the synthesis of (**5a**–**5e**) (lit. [25])*

*2.3.4.1. 1-Ethyl-5-phenylindolin-2-one **5a**.* A mixture of $K_2CO_3$ (2.12 g, 20 mmol), Pd $(OAc)_2$ (10 mg, 0.5 mol %), 5-bromo-N-ethyloxindole (2.4 g, 10 mmol), benzeneboronic acid (3 g, 15 mmol), distilled water (35 mL) and DMF (30 mL) was stirred under nitrogen for 48 h. Afterward, the reaction solution was extracted four times with diethyl ether (4 × 30 mL). The combined organic layers were washed with water, dried over anhydrous sodium sulfate. The product was then dried under high vacuum. The further purification of the product was achieved by flash chromatography on a silica gel column. Yield was 80.4% as yellow solid; m.p. 110–111 °C. $^1$H NMR ($CDCl_3$, 300 MHz): $\delta$ (ppm): 7.49–7.56 (m, 4H), 7.40–7.45 (m, 2H), 7.30–7.35 (m, 1H), 6.90 (d, 1H, $J$ = 8.3 Hz), 3.80–3.83 (m, 2H), 3.58 (s, 2H), 1.30 (t, 3H, $J$ = 7.2 Hz). $^{13}$C NMR (100 MHz, $CDCl_3$): $\delta$ (ppm) = 174.66, 143.71, 140.92, 135.66, 128.82, 126.95, 126.80, 126.70, 125.35, 123.49, 108.36, 35.98, 34.78, 12.73. Aal. Calcd. (%) for $C_{16}H_{15}N$: C, 80.98; H, 6.37; N, 5.90. Found: C, 80.92; H, 6.39; N, 5.88.

*2.3.4.2. 5-(4-tert-Butylphenyl)-1-ethylindolin-2-one **5b**.* Compound **5b** was synthesized according to the method described for compound **5a**. Yield was 78.6% as yellow solid; m.p. 125–127 °C. $^1$H NMR ($CDCl_3$, 300 MHz): $\delta$ (ppm): 7.50–7.43 (m, 6H), 6.90 (d, 1H, $J$ = 8.3 Hz), 3.77–3.79 (m, 2H), 3.58 (s, 2H), 1.39 (s, 9H), 1.31 (t, 3H, $J$ = 7.2 Hz). $^{13}$C NMR (100 MHz, $CDCl_3$): $\delta$ (ppm) = 174.67, 149.96, 143.46, 137.99, 135.51, 126.50, 126.42, 125.76, 125.27, 123.33, 108.33, 35.98, 34.76, 34.50, 31.36, 12.73. Aal. Calcd. (%) for $C_{20}H_{23}N$: C, 81.87; H, 7.90; N, 4.77. Found: C, 81.85; H, 7.95; N, 4.75.

*2.3.4.3. 1-Ethyl-5-(4-methoxyphenyl)indolin-2-one **5c**.* Compound **5c** was synthesized according to the method described for compound **5a**. Yield was 76.4% as yellow solid; m.p. 122–123 °C. $^1$H NMR ($CDCl_3$, 300 MHz): $\delta$ (ppm): 7.49–7.46 (m, 4H), 6.97 (d, 2H, $J$ = 8.5 Hz), 6.88 (d, 1H, $J$ = 8.8 Hz), 3.85 (s, 3H), 3.75–3.78 (m, 2H), 3.57 (s, 2H), 1.29 (t, 3H, $J$ = 7.2 Hz). $^{13}$C NMR (100 MHz, $CDCl_3$): $\delta$ (ppm) = 174.63, 158.92, 143.18, 135.35, 133.52, 127.80, 126.19, 125.32, 123.15, 114.26, 108.33, 55.35, 35.98, 34.76, 12.73. Aal. Calcd. (%) for $C_{17}H_{17}N$: C, 76.38; H, 6.41; N, 5.24. Found: C, 76.35; H, 6.39; N, 5.25.

*2.3.4.4. 5-(9,9-Dibutyl-9H-fluoren-2-yl)-1-ethylindolin-2-one **5d**.* Compound **5d** was synthesized according to the method described for compound **5a**. Yield was 63.7% as light yellow solid; m.p. 101–103 °C. $^1$H NMR ($CDCl_3$, 500 MHz): $\delta$ (ppm): 7.72 (m, 2H), 7.57 (d, 2H, $J$ = 7.8 Hz), 7.52 (q, 1H, $J$ = 8.2 Hz), 7.49 (s, 1H), 7.28–7.36 (m, 4H), 6.93 (d, 1H), 3.80–3.84 (m, 2H), 3.60 (s, 2H), 2.00 (t, 4H, $J$ = 8.3 Hz), 1.31 (t, 4H, $J$ = 8.2 Hz), 1.24 (t, 3H, $J$ = 7.2 Hz), 1.04–1.10 (m, 6H), 0.66–0.72 (m, 4H). $^{13}$C NMR (100 MHz, $CDCl_3$): $\delta$ (ppm) = 174.70, 151.47, 150.87, 143.56, 140.72, 140.16, 139.74, 136.16, 127.00, 126.81, 126.74, 126.74, 125.58, 125.39, 123.57, 122.89, 121.11, 119.95, 119.67, 108.38, 55.06, 40.25, 36.03, 34.82, 25.99, 23.08, 13.82, 12.74. Aal. Calcd. (%) for $C_{31}H_{35}NO$: C, 85.08; H, 8.06; N, 3.20. Found: C, 85.10; H, 8.03; N, 3.18.

*2.3.4.5. 5-(4-(Diphenylamino)phenyl)-1-ethylindolin-2-one **5e**.* Compound **5e** was synthesized according to the method described for compound **5a**. Yield was 70.3% as light yellow solid; m.p. 171–173 °C. $^1$H NMR ($CDCl_3$, 500 MHz): $\delta$ (ppm): 7.46 (d, 2H, $J$ = 7.5 Hz), 7.41 (d, 2H, $J$ = 8.6 Hz), 7.24–7.27 (m, 6H), 7.12 (d, 6H, $J$ = 7.5 Hz), 7.02 (t, 2H, $J$ = 7.4 Hz), 6.88 (d, 1H, $J$ = 8.6 Hz), 3.77–3.81 (m, 2H), 3.56 (s, 2H), 1.29 (t, 3H, $J$ = 7.0 Hz). $^{13}$C NMR (100 MHz, $CDCl_3$): $\delta$ (ppm) = 174.64, 147.66, 146.89, 143.30, 135.18, 134.89, 129.26, 127.40, 126.17, 125.32, 124.35, 124.03, 123.05, 122.90, 108.35, 35.98, 34.77, 12.73. Aal. Calcd. (%) for $C_{28}H_{24}N_2O$: C, 83.14; H, 5.98; N, 6.93. Found: C, 83.09; H, 5.99; N, 6.94.

*2.3.5. General procedure for the synthesis of (**1a**–**1e**) (lit. [21])*

*2.3.5.1. 5,10,15-Triethyl-3,8,13-triphenyl-10,15-dihydro-5H-diindolo [3,2-a:3′,2′-c] carbazole **1a**.* A mixture of **5a** (1.19 g, 5 mmol), $POCl_3$ (10 mL) and methylbenzene (20 mL) was stirred and refluxed for 24 h. After cooling, the mixture was poured into ice water, and then

extracted with DCM (100 mL) for three times. The combined organic layers were washed with water, dried over anhydrous sodium sulfate. The product was then dried under high vacuum, purified on a silica gel column using DCM/PE = 1/4, as eluent. A white solid **1a** (0.43 g, 39% yield) was obtained; m.p. 254 °C. $^1$H NMR (DMSO, 500 MHz) δ (ppm): 8.57 (s, 1H), 7.96 (d, 1H, $J$ = 8.5 Hz), 7.84 (d, 2H, $J$ = 7.4 Hz), 7.80 (d, 1H, $J$ = 8.4 Hz), 7.56 (t, 2H, $J$ = 7.5 Hz), 7.40 (t, 1H, $J$ = 7.3 Hz), 5.10–5.14 (m, 2H), 1.62 (t, 3H, $J$ = 6.9 Hz). $^{13}$C NMR (100 MHz, $CDCl_3$): δ (ppm) = 142.70, 140.36, 139.17, 133.42, 128.89, 127.41, 126.48, 123.95, 122.60, 120.38, 110.48, 103.48, 41.99, 15.82. Aal. Calcd. (%) for $C_{48}H_{39}N_3$: C, 87.64; H, 5.98; N, 6.39. Found: C, 87.70; H, 5.89; N, 6.37.

*2.3.5.2. 3,8,13-tris(4-tert-Butylphenyl)-5,10,15-triethyl-10,15-dihydro-5H-diindolo [3,2-a:3′,2′-c]carbazole **1b**.* Compound **1b** was synthesized according to the method described for compound **1a**. Yield was 40.5% as white solid; m.p. 254 °C. $^1$H NMR ($CDCl_3$, 500 MHz): δ (ppm): 8.57 (s, 1H), 7.68–7.71 (m, 4H), 7.52–7.55 (m, 2H), 5.04–5.08 (m, 2H), 1.70 (t, 3H, $J$ = 6.9 Hz), 1.41 (s, 9H). $^{13}$C NMR (100 MHz, $CDCl_3$): δ (ppm) = 149.39, 140.22, 139.77, 133.21, 126.99, 125.85, 123.95, 122.49, 120.18, 110.41, 103.50, 41.98, 34.53, 31.46, 26.91, 15.86. Aal. Calcd. (%) for $C_{60}H_{63}N_3$: C, 87.23; H, 7.69; N, 5.09. Found: C, 87.17; H, 7.75; N, 5.01.

*2.3.5.3. 5,10,15-Triethyl-3,8,13-tris(4-methoxyphenyl)-10,15-dihydro-5H-diindolo [3,2-a:3′,2′-c]carbazole **1c**.* Compound **1c** was synthesized according to the method described for compound **1a**. Yield was 33.7% as light yellow solid; m.p. 367 °C. $^1$H NMR ($CDCl_3$, 500 MHz): δ (ppm): 8.52 (s, 1H), 7.65–7.69 (m, 4H), 7.06–7.08 (m, 2H), 5.07–5.09 (m, 2H), 3.90 (s, 3H), 1.70 (t, 3H, $J$ = 6.9 Hz). $^{13}$C NMR (75 MHz, $CDCl_3$): δ (ppm) = 158.66, 140.08, 139.18, 135.38, 133.14, 128.36, 124.01, 122.30, 119.96, 114.37, 110.43, 103.52, 56.05, 41.97, 15.83. Aal. Calcd. (%) for $C_{51}H_{45}N_3O_3$: C, 81.90; H, 6.06; N, 5.62. Found: C, 81.20; H, 6.11; N, 5.58.

*2.3.5.4. 3,8-bis(9,9-Dibutyl-9H-fluoren-2-yl)-13-(9,9-dibutyl-9H-fluoren-3-yl)-5,10,15-triethyl-10,15-dihydro-5H-diindolo[3,2-a:3′,2′-c] carbazole **1d**.* Compound **1d** was synthesized according to the method described for compound **1a**. Yield was 31.6% as white solid; m.p. 219 °C. $^1$H NMR ($CDCl_3$, 500 MHz): δ (ppm): 8.68 (s, 1H), 7.80–7.85 (m, 2H), 7.75–7.79 (m, 4H), 7.31–7.40 (m, 3H), 5.13–5.15 (m, 2H), 2.06–2.10 (m, 4H), 1.85 (t, 3H, $J$ = 7.0 Hz), 1.10–1.18 (m, 4H), 0.71–0.78 (m, 10H). $^{13}$C NMR (75 MHz, $CDCl_3$): δ (ppm) = 151.48, 150.88, 141.54, 140.97, 140.43, 139.71, 139.32, 134.02, 127.36, 126.85, 126.81, 126.20, 124.05, 122.88, 122.73, 121.77, 120.31, 120.00, 119.63, 110.45, 103.51, 55.09, 42.10, 40.43, 26.06, 23.15, 16.05, 13.85. Aal. Calcd. (%) for $C_{93}H_{99}N_3$: C, 88.73; H, 7.93; N, 3.34. Found: C, 88.61; H, 7.96; N, 3.39.

*2.3.5.5. 4,4′-(13-(3-(Diphenylamino)phenyl)-5,10,15-triethyl-10,15-dihydro-5H- diindolo[3,2-a:3′,2′-c]carbazole-3,8-diyl)bis(N,N-diphenylaniline) **1e**.* Compound **1e** was synthesized according to the method described for compound **1a**. Yield was 28.6% as light yellow solid. m.p. 372 °C. $^1$H NMR ($CDCl_3$, 400 MHz): δ (ppm): 8.55 (s, 1H), 7.64–7.68 (m, 4H), 7.18–7.31 (m, 9H), 7.02–7.06 (m, 3H), 5.05–5.01 (m, 2H), 1.70 (t, 3H, $J$ = 7.2 Hz). $^{13}$C NMR (75 MHz, $CDCl_3$): δ (ppm) = 147.84, 146.48, 140.16, 139.14, 136.78, 132.86, 129.26, 129.12, 127.91, 124.36, 124.01, 122.77, 122.21, 119.79, 110.48, 103.55, 41.99, 15.81. Aal. Calcd. (%) for $C_{84}H_{66}N_6$: C, 87.01; H, 5.74; N, 7.25. Found: C, 87.09; H, 5.61; N, 7.22.

## 3. Results and discussion

### 3.1. Synthesis and characterization

The synthesis of 3,8,13-substituted triindole derivatives **1a**–**1e** was carried out by using a multi-step synthetic route, as shown in Scheme 1. As a key compound, 5-bromo-N-ethyloxindole **3** was extracted from the monobromination of N-ethyloxindole **2**, which was obtained through the synthesis starting from *N*-ethylaniline [21]. The aryl boronic acids **4a**–**4e**, as other key compounds, were obtained by following a similar procedure (Scheme 2). **4a**–**4c** were easily be synthesized by the treatment of the corresponding aryl Grignard compounds with trimethyl borate [22]. **4d** and **4e** were achieved in a two-step synthesis: lithiation arylhalide with an excess of *n*-BuLi was followed by treatment of trimethyl borate, Suzuki cross-coupling of aryl boronic acids **4a**–**4e** and 5-bromo-N-ethyloxindole **3**, using Pd $(OAc)_2$ as catalyst, afforded 3-substituted indolin-2-one derivatives **5a**–**5e** in quantitative yields [25]. Trimerization of **5a**–**5e** in $POCl_3$ yielded the desired products **1a**–**1e** in 29.8%–40.5% yields, which are similar with the yields reported by the unsubstituted triindole core [19]. Triphenylamino substituted **1e** has the least number of yields among these compounds. The results demonstrate that triindole derivatives can be synthesized directly by trimerization of aryl derivatives of indolin-2-one.

The synthesized compounds **1a**–**1e** were identified by using the $^1$H NMR spectra, $^{13}$C NMR spectra, and element analysis. The data were found to be in good agreement with the proposed structures. The compounds **1a**–**1e** were soluble in common organic solvents, such as DCM, $CH_3CN$, THF, etc., at room temperature.

### 3.2. Thermal properties

Table 1 shows the thermal properties, including melting and decomposition temperatures, of these molecules. Differential scanning calorimetry (DSC) was used to investigate the phase transitions. No glass transition events were observed by the DSC scans of the molecules. All compounds had melting transitions ranging from 219 °C to 373 °C. Fluorenyl substituted **1d** melting at the lowest temperature of 219 °C, while triphenylamino substituted **1e** melting at the highest temperature, 373 °C. The decomposition temperatures determined by the thermogravimetric analysis (TGA) were above 405 °C (Fig. 1). All these results demonstrated that the series of 3,8,13-substituted triindole derivatives were very robust molecules.

### 3.3. X-ray crystal structures

Crystal **5e** was grown by the slow evaporation of its solution in PE at room temperature. The diffraction data of a crystal were collected at 298 K. The crystal structure was solved by using direct methods, and refined by applying full-matrix least-squares techniques implemented in the SHEXTL crystallographic software [28,29]. The crystal belongs to the monoclinic system, $P2_1/n$ space group with formula $C_{28}H_{24}N_2O$; $a$ = 9.2810(19), $b$ = 15.884(3), $c$ = 14.752(3) Å; $\beta$ = 90.30(3)°; $V$ = 2174.7(8) Å$^3$; $\rho_{cal}$ = 1.235 g/cm$^3$, $\mu$ = 0.075 mm$^{-1}$. All H atoms were clearly located in the different Fourier maps and were refined freely. The refinement converged to $R1$ = 0.1933, $wR2$ = 0.1405, $\rho_{max}$ = 0.144 e/Å$^3$, $\rho_{min}$ = −0.176 e/Å$^3$. The detailed crystallographic data for **5e** are presented in Table 2.

The single crystal structures and packing diagrams of **5e** are shown in Figs. 2 and 3, respectively. As shown in Fig. 2, **5e** consists

**Table 1**
Thermal properties of **1a**–**1e**.

| Compd. | $T_m$ (°C) | $T_d$ (°C) |
|---|---|---|
| **1a** | 254 | 405 |
| **1b** | 254 | 420 |
| **1c** | 368 | 448 |
| **1d** | 219 | 429 |
| **1e** | 373 | 438 |

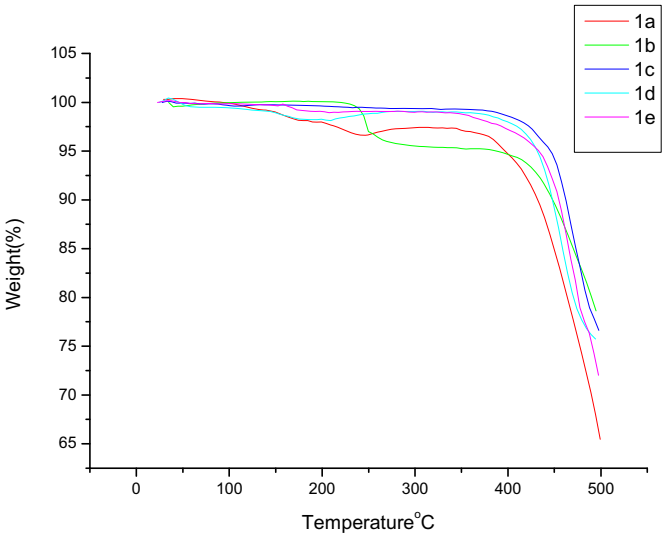


**Fig. 1.** TGA curves of **1a**–**1e**.

of indole and triphenylamine moieties. The crystal structures reveal that the indole units are relatively planar. The a-linked phenyl groups are twisted at 32.4° in **5e** from the plane of the indole units. At the triphenylamine moiety, the central nitrogen and its three bended carbon atoms are coplanar, which form a quasi-equilateral trigonal NC3 plane with the sum of the three C–N–C angles (360.0°). Around the central nitrogen, three phenyl ring planes are arranged in a propeller-like fashion.

### 3.4. Optical properties

The absorption and emission spectra of **1a**–**1e** recorded from dilute DCM solutions ($1 \times 10^{-6}$ M) and thin films are shown in Figs. 4–7. Table 3 shows the absorption peak wavelengths ($\lambda_{max}^{Abs}$),

**Table 2**
Crystallographic data for **5e**.

| | |
|---|---|
| Compound | **5e** |
| Chemical formula | $C_{28}H_{24}N_2O$ |
| Formula weight | 404.49 |
| Crystal system | Monoclinic |
| Space group | P21/N |
| $a$ (Å) | 9.2810(19) |
| $b$ (Å) | 15.884(3) |
| $c$ (Å) | 14.752(3) |
| $\alpha$ (°) | 90.00 |
| $\beta$ (°) | 90.30(3) |
| $\gamma$ (°) | 90.00 |
| $V$ (Å$^3$) | 2174.7(8) |
| $D_{calc}$ (g cm$^{-3}$) | 1.235 |
| $\mu$ (mm$^{-1}$) | 0.075 |
| $F$ (000) | 856 |
| $\theta$ range (°) | 1.88–25.38 |
| Index range | $0 \le h \le 11$<br>$0 \le k \le 19$<br>$-17 \le l \le 17$ |
| Reflns collected | 4255 |
| Unique reflns ($R_{int}$) | 3996 (0.085) |
| Refinement method on $F^2$ | Full-matrix least-squares |
| GOF on $F^2$ | 1.002 |
| $R_1$ [$I > 2\sigma$ ($I$)] | 0.0782 |
| $wR_2$ [$I > 2\sigma$ ($I$)] | 0.1092 |
| $R_1$ (all data) | 0.1933 |
| $wR_2$ (all data) | 0.1405 |
| Residual (e Å$^{-3}$) | 0.144 and −0.176 |

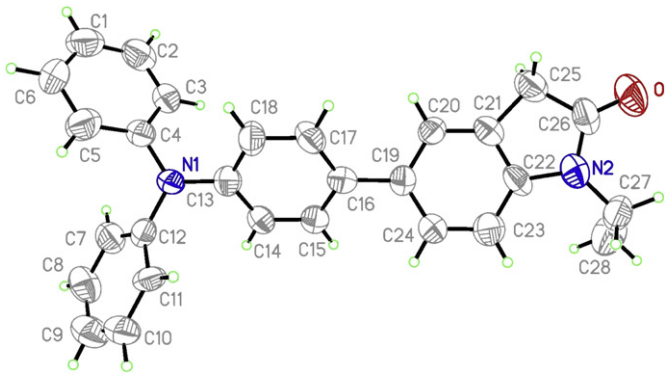


**Fig. 2.** The crystal structure of **5e**.

optical band gaps ($E_g$), photoluminescence (PL) peak wavelengths, ($\lambda_{max}^{Em}$), quantum yields in solution, and solid-state.

Based on the electronic absorption spectra of **1a**–**1e** in dilute DCM solutions (Fig. 4), these triindoles exhibit strong π–π* electron absorption bands, with two characteristic absorption peaks, one at 311, 312, 281, 321 and 323 nm, and the other at 332, 334, 311, 344, and 345 nm. Phenyl substituted **1a**, alkyl phenyl substituted **1b**, and methoxyl substituted **1c** have nearly identical absorption maxima ($\lambda_{max}^{Abs}$) at 311, 312, and 311 nm, respectively. The increase in conjugation length and electron density associated with fluorenyl groups in **1d**, and triphenylamino groups in **1e** led to a large bathochromic shift of absorption maximum in **1d** to 344 nm, and in **1e** to 345 nm.

The solid-state optical absorption spectra of compounds **1a**–**1e** are shown in Fig. 5. **1a**–**1e** exhibit a strong π–π* transition at 371, 371, 371, 386, and 391 nm. Regarding the absorption spectra of **1a**–**1e** in films (Fig. 4), the trends observed with extending the conjugation upon functionalization in terms of the spectral shapes and peak positions are nearly the same compared to the spectra we obtained in dilute solutions.

The photoluminescence (PL) spectra of the derivatives **1a**–**1e** in dilute DCM solutions ($1 \times 10^{-7}$ M) are shown in Fig. 6. **1a**–**1c** exhibit similar PL spectra with the main emission peak and the shoulder emission peak in solution. The emission peak ranges from 406 to 407 nm with a Stokes shift of approximately 95 nm. The $\lambda_{max}^{Em}$ of fluorenyl substituted **1d** slightly red shifted (6 nm) compared to **1a**. However, the $\lambda_{max}^{Em}$ of triphenylamino substituted **1e** has slightly blue shifted (12 nm) compared to **1a**. A Stokes shift of 68 and 49 nm are shown by **1d** and **1e**, respectively. These experimental data clearly indicate that the substitutions exerted little considerable influence on the electronic states in solution. The large Stokes shifts between 49 and 95 nm observed for **1a**–**1e** are the consequences of both the nuclear reorganization that takes place after the prior emission and irradiation, which results from the conformational changes and electronic redistribution in the phenyl fragments (planarization) upon excitation [30].

The emission spectra of **1a**–**1e** in film are shown in Fig. 7. All five compounds emit blue light with the emission maximum ranging from 416 nm, for **1a**, to 461 nm for **1d**. All the $\lambda_{max}^{Em}$ of **1b**–**1e** are slightly red shifted compared to **1a**. Fluorenyl substituted **1d** has the maximum red shift (44.5 nm). The Stoke shifts are not very large for all compounds ranging from 45 to 76 nm.

Optical band gaps ($E_g^{opt}$) determined from the absorption edge of the solution and the solid-state spectra are shown in Table 3. The optical band gap varies from 3.07 to 3.17 eV for **1a**–**1e** in solution and from 2.43 to 2.67 eV for **1a**–**1e** in solid-state.

The fluorescence quantum efficiencies ($\Phi_f^a$) of **1a**–**1e** were measured in dilute DCM solutions using 9,10-diphenylanthracene

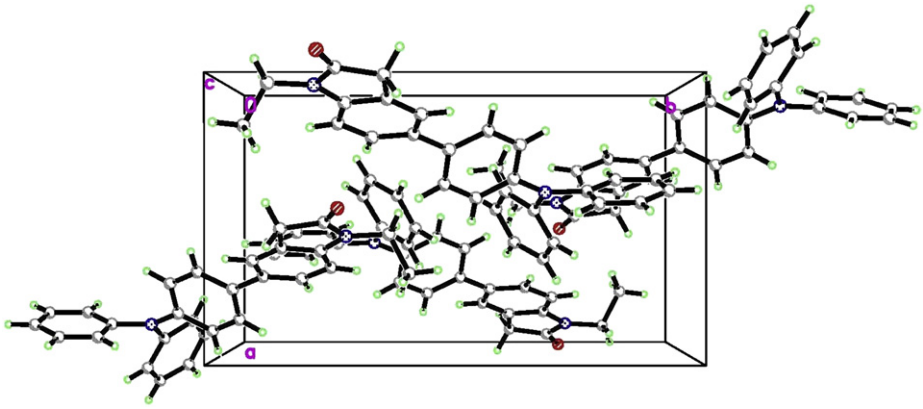

**Fig. 3.** Crystal packing diagram of **5e**.

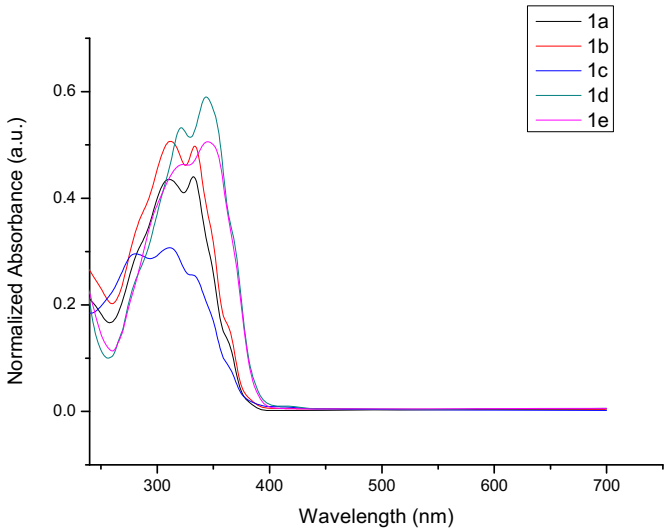


**Fig. 4.** UV–Vis absorption spectra of **1a**–**1e** in DCM solution ($1 \times 10^{-6}$ M).

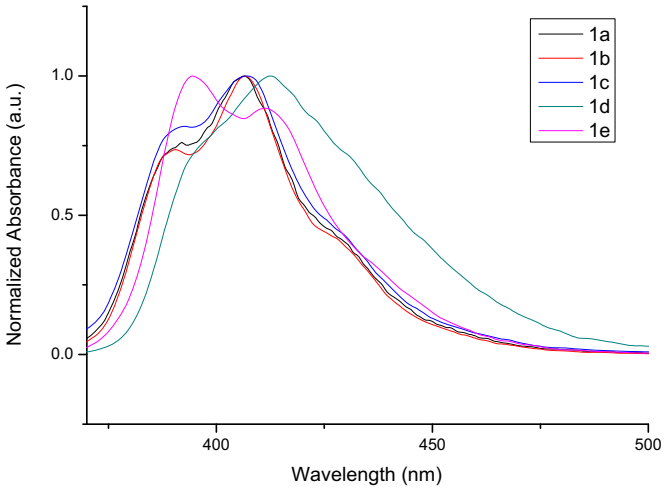


**Fig. 6.** PL spectra of **1a**–**1e** in DCM solution ($1 \times 10^{-7}$ M).

($\Phi_f^a = 0.91$ in ethanol) as a standard [31]. The quantum efficiencies of **1a**–**1e** ranged from 0.32 to 0.58 in DCM solutions (Table 3). There was only a small difference in $\Phi_f^a$ between **1a**, **1b**, and **1c**. Fluorenyl substituted **1d** obviously increased in fluorescence quantum efficiencies. However, **1e** showed low fluorescence quantum efficiencies and it is likely that triphenylamino effect is little in luminescence intensity. From among the five compounds synthesized, **1d** showed the highest fluorescence quantum efficiencies (0.58) and the largest $\lambda_{max}^{Em}$ (412 nm) with high thermal stability

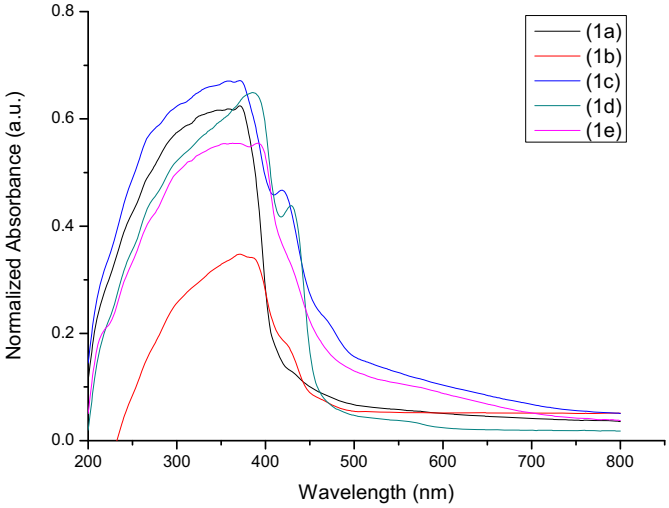


**Fig. 5.** UV–Vis absorption spectra of **1a**–**1e** in the solid state.

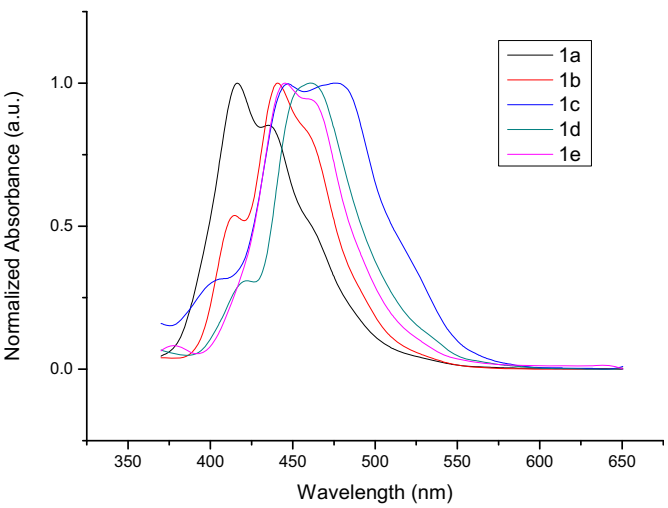


**Fig. 7.** PL spectra of **1a**–**1e** in the solid state.

**Table 3**
UV absorption and PL properties of **1a**–**1e** in DCM solution and solid film.

| Compd. | $\lambda_{max}^{Abs}$ (nm) | $\lambda_{max}^{Em}$ (nm) | Stokes shift (nm) | $E_g^{opt}$ (eV) | $\Phi_f^a$ |
|---|---|---|---|---|---|
| | Solution/solid | Solution/solid | Solution/solid | Solution/solid | |
| **1a** | 311/371 | 406/416 | 95/45 | 3.17/2.67 | 0.32 |
| **1b** | 312/371 | 406/441 | 94/70 | 3.14/2.63 | 0.36 |
| **1c** | 311/371 | 407/447 | 96/76 | 3.14/2.64 | 0.27 |
| **1d** | 344/386 | 412/461 | 68/75 | 3.07/2.54 | 0.58 |
| **1e** | 345/391 | 394/445 | 49/49 | 3.10/2.43 | 0.37 |

[a] Fluorescence quantum efficiency, relative to 9,10-diphenylanthracene in ethanol ($\Phi_f = 0.91$).

($T_m$ = 219 °C, $T_d$ = 429 °C). This compound is expected to be applicable as a blue light emitting material.

### 3.5. Electrochemical properties

The electrochemical behavior of **1a**–**1e** was investigated by using a cyclic voltammetry (CV) in $c = 10^{-3}$ mol $L^{-1}$ in $CH_2Cl_2$ and 0.1 M tetra-n-butylammonium hexafluorophosphate (TBAP) using a Pt working electrode. Measurements were performed at room temperature under nitrogen with a scanning rate of 40 mV/s and SCE energy level of 4.4 eV vs vacuum [26,32]. Therefore, the HOMO and lowest unoccupied molecular orbital (LUMO) energy levels as well as the energy gap of these compounds can be estimated using the following equations:

$$EA(LUMO) = E_{red}^{onset} + 4.4\ eV \quad (1)$$

$$IP(HUMO) = E_{ox}^{onset} + 4.4\ eV \quad (2)$$

$$E_g^{el} = E_{ox}^{onset} - E_{red}^{onset} \quad (3)$$

where $E_{ox}^{onset}$ and $E_{red}^{onset}$ are the onset potentials for oxidation and reduction relative to the $Ag/Ag^+$ reference electrode.

As seen from Fig. 8, all figures show the first reduction peak ranging from −0 V to −0.34 V because of the impact of DCM. The molecules of **1a** have only one reduction peak, whereas molecules **1b**, **1c**, **1d**, and **1e** have two reduction peaks. **1e** only has one peak,

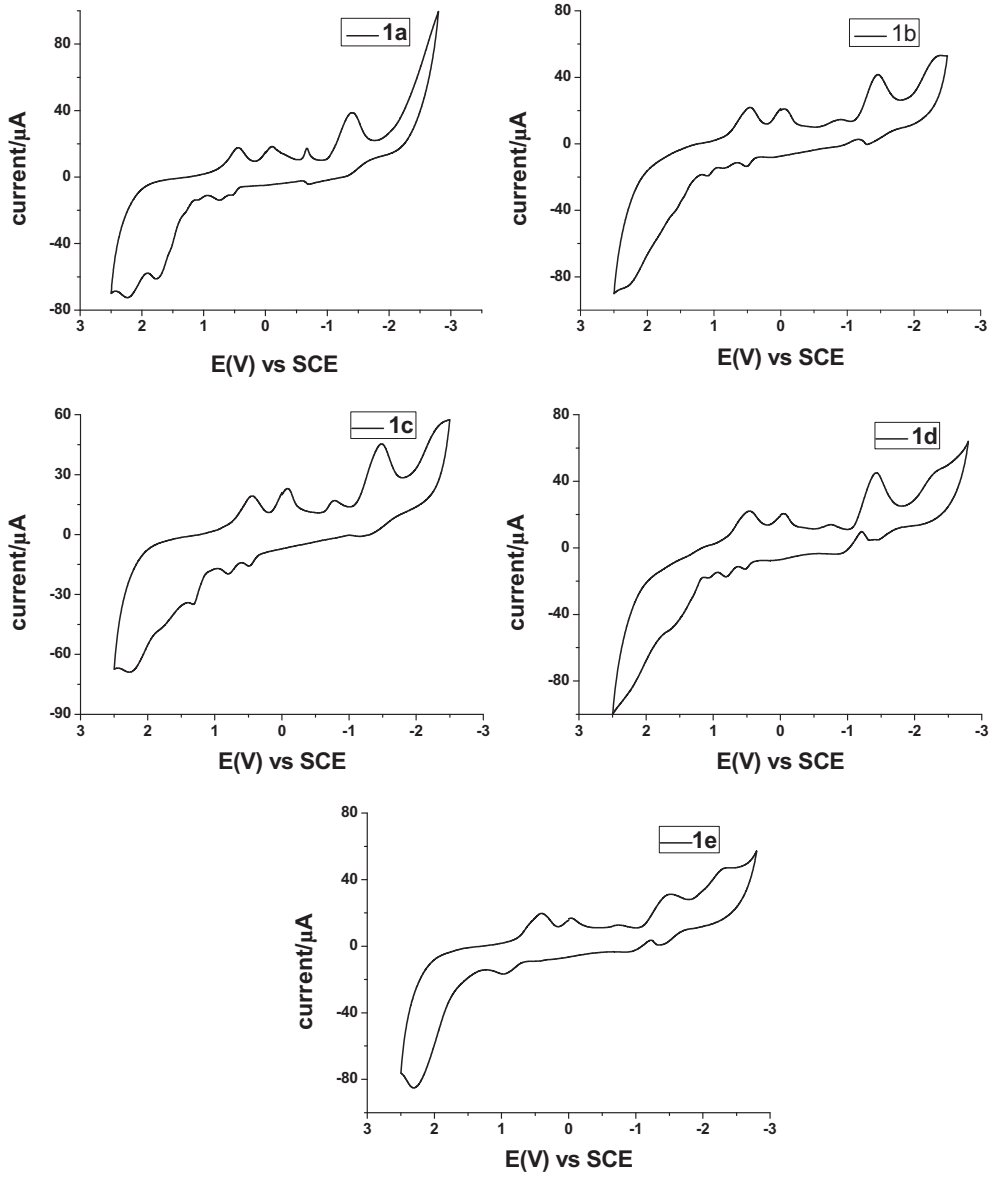


**Fig. 8.** Cyclic voltammograms of thin films of **1a**–**1e** coated on a Pt wire electrode. Scan rate 40 mV/s.

**Table 4**
Electrochemical properties of **1a**–**1e**.[a]

| Compd. | $E_{red}^{onset}$ (V) | EA[b] (eV) | $E_{ox}^{onset}$ (V) | IP[b] (eV) | $E_g^{el}$ (eV) |
|---|---|---|---|---|---|
| **1a** | −0.69 | 3.71 | 0.72 | 5.12 | 1.41 |
| **1b** | −0.86 | 3.54 | 1.08 | 5.48 | 1.94 |
| **1c** | −0.80 | 3.60 | 0.78 | 5.28 | 1.58 |
| **1d** | −0.77 | 3.63 | 0.77 | 5.17 | 1.54 |
| **1e** | −0.76 | 3.66 | 0.95 | 5.35 | 1.71 |

[a] All potentials vs SCE reference.
[b] EA (LUMO) = $E_{red}^{onset}$ + 4.4 eV; IP (HOMO) = $E_{ox}^{onset}$ + 4.4 eV; $E_g^{el}$ = IP − EA.

whereas there were two irreversible oxidation peaks in **1a**, **1b**, **1c**, and **1d**.

As shown in Table 4, **1a**–**1e** have electron affinities (LUMO) between 3.54 and 3.71 eV (below vacuum), which reveal promising electron-transport properties for OLEDs. The reduction potentials of all the molecules were relatively unchanged by the substituents (R groups), which indicate that the electron affinities (LUMO) lied on the 10,15-dihydro-5H-diindolo [3,2-a:30,20-c] carbazole moiety. Even the electron-rich fluorene substituted molecule (**1d**), which had expectedly the lowest oxidation potential, had essentially the same LUMO level as the other molecules.

The formal reduction potential ($E_{red}^{onset}$) varies from −0.69 V (vs SCE), for **1a** to −0.86 V, for **1b** (Table 4). As a result, the estimated ionization potential (HOMO) is reduced from 5.48 eV in **1b** to 5.12 eV in **1a**, which suggesting a significant lowering of the energy barrier for hole injection from the indium tin oxide (ITO)/poly(3,4-ethylenedioxythiophene) doped with poly-(styrenesulfonate) (PEDOT:PSS) anode (work function = −5.2 eV) [18]. The electrochemically derived band gap ($E_g^{el}$) of **1a**–**1e** is shown in Table 4. $E_g^{el}$ varies from 1.41 eV for **1a** to 1.94 eV for **1b**. From the five compounds synthesized, **1d** shows high HOMO energy level (5.48 eV), lowest LUMO level (3.54 eV), and wide $E_g^{el}$ value (1.94 eV). These characteristics suggest that **1a**–**1e** has the potential to be used as material for hole-transport and injection in OLEDs [33].

### 3.6. Theoretical calculation

Quantum chemical calculations were performed to determine the electronic properties and the geometries of the 3,8,13-substituted triindole derivatives. In the calculations, the ground state geometries of **1a**–**1e** were fully optimized by using density functional theory (DFT) at the B3LYP/6-31G level, as implemented in the Gaussian 03. DFT/B3LYP calculation of lowest excitation energies was performed at the optimized geometries of the ground states. The optimized structures of all the compounds (**1d** as an example, Fig. 9) reveal that the substituted moieties attached to all ends of the molecule are nearly coplanar with the triindole backbone. Therefore, π-electron delocalization between those units is unlikely to be negligible. In their HOMO orbitals (Fig. 10), the π-electrons are able to delocalize over the entire triindole backbone and one end-capped moiety. The LUMO is delocalized through the triindole backbone and two end-capped moieties, as illustrated in Fig. 10. Therefore, a significant change in charge distribution would result in the HOMO-LUMO transition in compounds **1a**–**1e**. The HOMO-LUMO energy differences (energy band gaps, calculated $E_g^{cal}$) at DFT/B3LYP level of theory are presented in Table 5. The result indicates that $E_g^{cal}$ values decrease as the length of π-conjugated system and the electron-donating ability of end-capped moieties increase. These predicted $E_g^{cal}$ values are higher than the estimated figures from the onset of UV–Vis absorption ($E_g^{opt}$) and

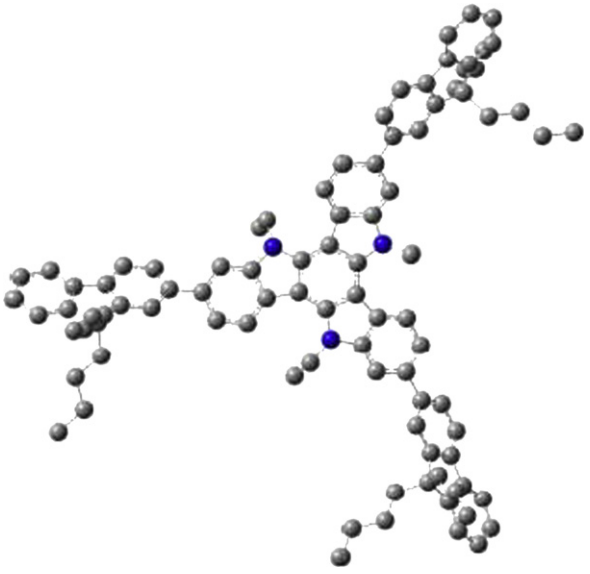

**Fig. 9.** B3LYP/6-31G optimized geometry of compound **1d**.

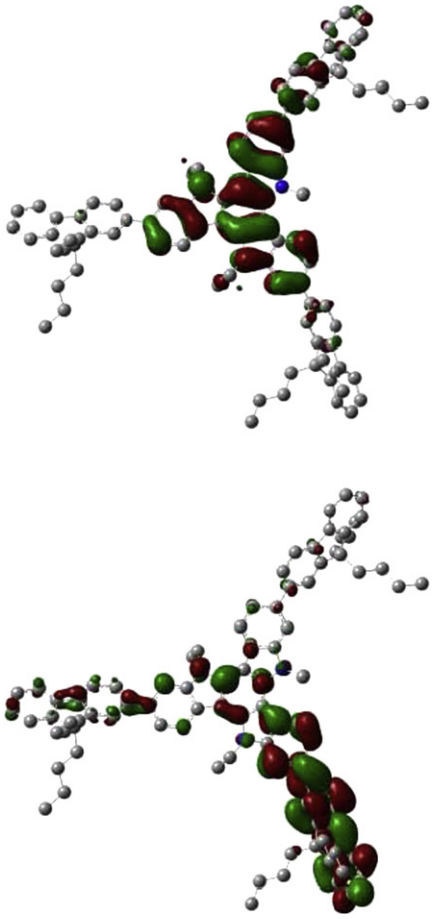

**Fig. 10.** HOMO (bottom) and LUMO (top) for molecules **1d** in gas phase.

**Table 5**
Energy values theoretically calculated for molecules **1a**–**1e** in gas phase.

| Compd. | Energy (eV) | | |
|---|---|---|---|
| | LUMO | HOMO | $E_g^{cal}$ |
| **1a** | −0.90 | −4.84 | 3.94 |
| **1b** | −0.83 | −4.77 | 3.94 |
| **1c** | −0.72 | −4.68 | 3.96 |
| **1d** | −1.10 | −4.78 | 3.68 |
| **1e** | −0.91 | −4.65 | 3.74 |

[cal]: Energies theoretically calculated for gas phase by means of DFT B3LYP/6-31G.

cyclic voltammograms ($E_g^{cal}$). Errors may be responsible for this finding because the orbital energy difference between HOMO and LUMO is still an approximate estimation to the transition energy. However, the transition energy contains significant contributions from two or three electron integrals. The real situation is that an accurate description of the lowest singlet excited state requires a linear combination of a number of excited configurations.

## 4. Conclusions

We have synthesized and investigated the thermal stabilities, electrochemical, and photophysical properties of five novel 3,8,13-substituted triindoles. These materials showed high thermal stability with high decomposition temperature (above 405 °C) and high melt transition (219 °C–373 °C). The molecule structure of the **5e** was characterized by using an X-ray analysis. The results showed that **5e** was crystallized in the triclinic system with the space group $P2_1/n$. Absorption and fluorescence spectral characteristics of the compounds were investigated in the DCM solution and solid film. Compared to **1a**, both the UV–Vis absorption maximum peaks (from 311 to 345 nm in DCM solution and from 371 to 391 nm in solid film) and PL emission peaks (from 394 to 412 nm in DCM solution and from 416 to 461 nm in solid film) slightly red shifted in **1b**–**1d**. Among the five compounds synthesized, **1d** has more potential to be used as a blue light emitting material. Based on the high-lying HOMO energy level, these compounds are expected to be promising hole-transport and injection materials for OLEDs with a wide band and reasonable electron and hole mobility.

## References


[1] Forrest SR, Thompson ME. Special issue on organic electronic and optoelectronics. Chem Rev 2007;107(4):923–1386.
[2] Weiss DS, Abkowitz M. Advances in organic photoconductor technology. Chem Rev 2010;110(1):479–526.
[3] Martin RE, Diederich F. Linear monodisperse π-conjugated oligomers: model compounds for polymers and more. Angew Chem Int Ed 1999;38(10):1350–77.
[4] Kraft A, Grimsdale AC, Holmes AB. Electroluminescent conjugated polymers-seeing polymers in a new light. Angew Chem Int Ed 1998;37(4):402–28.
[5] Gustafsson G, Cao Y, Treacy GM, Klavetter F, Colaneri N, Heeger AJ. Flexible light-emitting diodes made from soluble conducting polymers. Nature 1992;357(11):477–9.
[6] Tang CW, VanSlyke SA. Organic electroluminescent diodes. Appl Phys Lett 1987;51(12):913–5.
[7] Redecker M, Bradley DDC, Inbasekaran M, Wu WW, Woo EP. High mobility hole transport fluorene-triarylamine copolymers. Adv Mater 1999;11(3):241–6.
[8] Zhou X, Blochwitz J, Pfeiffer M, Nollau A, Fritz T, Leo K. Enhanced hole injection into amorphous hole-transport layers of organic light-emitting diodes using controlled p-type doping. Adv Funct Mater 2001;11(4):310–4.
[9] Ikai M, Tokito S, Sakamoto Y, Suzuki T. Highly efficient phosphorescence from organic light-emitting devices with an exciton-block layer. Appl Phys Lett 2001;79(2):156–9.
[10] Zang L, Che Y, Moore JS. One-dimensional self-assembly of planar π-conjugated molecules: adaptable building blocks for organic nanodevices. Acc Chem Res 2008;41(12):1596–608.
[11] Schenning APH, Meijer EW. Supramolecular electronics; nanowires from self-assembled π-conjugated systems. Chem Commun 2005;41(26):3245–58.
[12] Wu J, Pisula W, Muellen K. Graphenes as potential material for electronics. Chem Rev 2007;107(3):718–47.
[13] Zhang Y, Wada T, Sasabe H. Carbazole photorefractive materials. J Mater Chem 1998;8(4):809–28.
[14] Grazulevicius JV, Strohriegel P, Pielichowski J, Pielichowski K. Carbazole-containing polymers: synthesis, properties and applications. Prog Polym Sci 2003;28(9):1297–353.
[15] Zhao B, Liu B, Png RQ, Zhang K, Lim KA, Luo J, et al. New discotic mesogens based on triphenylene-fused triazatruxenes: synthesis, physical properties, and self-assembly. Chem Mater 2010;22(9):435–49.
[16] Talarico M, Termine R, Garcia-Frutos EM, Omenat A, Serrano JL, Gomez-Lor B, et al. New electrode-friendly triindole columnar phases with high hole mobility. Chem Mater 2008;20(21):6589–91.
[17] Garcia-Frutos EM, Gutierrez-Puebla E, Monge MA, Remirez R, Andres P, Andres A, et al. Crystal structure and charge-transport properties of *n*-trimethyltriindole: novel p-type organic semiconductor single crystals. Org Electron 2009;10(4):643–52.
[18] Lai WY, He QY, Zhu R, Chen QQ, Huang W. Kinked star-shaped fluorene/triazatruxene co-oligomer hybrids with enhanced functional properties for high-performance, solution-processed, blue organic light-emitting diodes. Adv Funct Mater 2008;18(2):265–76.
[19] Hiyoshi H, Kumagai H, Ooi H. Substituted sym-triindole. Pat. Appl. Publ. WO2005077956; 2005.
[20] Garcia-Frutos EM, Gomez-Lor B, Monge A, Gutierrez-Puebla E, Alkorta I. Synthesis and preferred all-*syn* conformation of $c_3$-symmetrical *n*-(hetero) arylmethyl triindoles. Chem Eur J 2008;14(18):8555–61.
[21] Ji L, Fang Q, Yuan MS, Liu ZQ, Shen YX, Chen HF. Switching high two-photon efficiency: from 3,8,13-substituted triindole derivatives to their 2,7,12-isomers. Org Lett 2010;12(22):5192–5.
[22] Miura Y, Oka H, Momoki M. A convenient and efficient synthesis of polyphenylmono-, di-, and -triaminobenzenes. Synthesis 1995;1995(11):1419–22.
[23] Li ZH, Wang MS, Tao Y, Lu JP. Diphenylamino end-capped oligofluorenes with enhanced functional properties for blue light emission: synthesis and structure–property relationships. Chem Eur J 2005;11(22):3285–93.
[24] Wang HY, Chen G, Xu XP, Chen H, Ji SJ. The synthesis and photophysical properties of novel poly(diarylamino)styrenes. Org Lett 2003;5(23):839–42.
[25] Liu LF, Zhang YH, Xin BW. Synthesis of biaryls and polyaryls by ligand-free Suzuki reaction in aqueous phase. J Org Chem 2006;71(10):3994–7.
[26] Agrawal AK, Jenekhe SA. Electrochemical properties and electronic structures of conjugated polyquinolines and polyanthrazolines. Chem of Mater 1996;8(2):579–89.
[27] Seaman W, Johnson JR. Derivatives of phenylboric acid, their preparation and action upon bacteria. J Am Chem Soc 1931;53(2):711–23.
[28] Sheldrick GM. SHELXL-97. Program for the refinement of crystal structures. Germany: University of Göttingen; 1997.
[29] Siemens. SHELXTL. Version 5.06. Madison, Wisconsin, USA: Siemens Analytical X-ray Instruments Inc; 1996.
[30] Mank D, Raytchev M, Amthor S, Lambert C, Fiebig T. Femtosecond probing of the excited state absorption and structural relaxation in biphenyl derivatives. Chem Phys Lett 2003;376(1–2):201–6.
[31] Eaton DF. International union of pure and applied chemistry organic chemistry division commission on photochemistry. Reference materials for fluorescence measurement. J Photochem Photobiol B 1988;2(4):523–31.
[32] Liu S, Jiang P, Song G, Liu R, Zhu H. Synthesis and optical properties of a series of thermally stable diphenylanthrazolines. Dyes Pigm 2009;81(3):218–23.
[33] Chiang CL, Shu CF. Synthesis and characterization of new polyquinolines containing 9,9′-spirobifluorene units. Chem Mater 2002;14(2):682–7.